

# Relationship Between Menard $E_M$ and Young's $E$ Moduli for Cohesionless Soils Relation entre le module pressiométrique Ménard $E_M$ et le module d'Young $E$ , pour les sols sans cohésion

G. Sedran

*In-Depth Geotechnical Inc., Hamilton, Ontario, Canada*

R. A. Failmezger

*In-situ Soil Testing L.C., Lancaster, Virginia, USA*

A. Drevininkas

*DownUnder Geotechnical Ltd., Maple, Ontario, Canada*

**ABSTRACT :** Pressuremeter testing (PMT) provides stress-strain data for both pseudo-elastic and elasto-plastic ranges of soil deformation. The Menard modulus  $E_M$  calculated as the slope of the pseudo-elastic portion of the  $p$  vs.  $\epsilon_R$  curve, measures elastic properties of the soil which are based on non-uniform stress and strain fields. As such  $E_M$  cannot directly be identified with the Young's modulus of the soil,  $E$ . The Menard's  $\alpha$  parameter is often used to estimate  $E$  from the measured  $E_M$ . Although practical, this empirical approach provides little insight into the interaction between the PMT probe and the surrounding soil. This paper explores back-calculating  $E_M$  of cohesionless soils knowing values of  $E$ , a priori. In this exercise, the behavior of soils under PMT testing conditions is modeled using finite element analysis (FEA) assuming uniform values of  $E$ . FEA predictions are then used to reconstruct pressuremeter  $p$  vs.  $\epsilon_R$  curves from which  $E_M$  is back-calculated. In a parametric approach, the relation between  $E_M$  and  $E$  is plotted for a range of soil stiffness  $E$  values, and a range of values of the in-situ horizontal stresses  $p_0$ . A relation between  $E_M$  and  $E$  for cohesionless soils is proposed.

**KEYWORDS :** in-situ testing; pressuremeter; elastic moduli; cohesionless soils; finite element analysis; back-calculation.

**RÉSUMÉ :** Le module pressiométrique Ménard  $E_M$  mesure des propriétés élastiques du sol qui se basent sur des champs de contraintes et de déformations non-uniformes. Le paramètre  $\alpha$  proposé par Ménard est souvent utilisé afin d'estimer le module de Young  $E$  à partir du module pressiométrique  $E_M$ . Bien que pratique, cette approche empirique fournit peu d'informations sur l'interaction entre la sonde pressiométrique et le sol avoisinant. Cet article explore le rétrocalcul de  $E_M$  pour des sols pulvérulents connaissant, a priori, les valeurs de  $E$ . Cette communication consiste à modéliser par méthode d'éléments finis (FEA) le comportement de sols soumis à des essais pressiométriques en assumant des valeurs uniformes de  $E$ . Les prédictions FEA sont alors utilisées pour tracer de nouvelles courbes pressiométriques  $p$  vs.  $\epsilon_R$  desquelles  $E_M$  est rétrocalculé. Dans une approche paramétrique, la relation entre  $E_M$  et  $E$  est tracée pour une gamme de valeurs de rigidité  $E$ , et pour une gamme de valeurs de contraintes horizontales in situ  $p_0$ . Une relation entre  $E_M$  et  $E$  est ainsi proposée pour des sols pulvérulents.

**MOTS-CLES :** essais in situ, pressiomètre, module élastique, sols pulvérulents, analyse par éléments finis, rétrocalcul.

## 1 INTRODUCTION

Loading conditions during pressuremeter testing (PMT) generate non-uniform stress and strain fields. This paper investigates the effects of non-uniform stress-strain distributions in the interpretation of soil properties from PMT testing.

While PMT stress-strain responses provide soil parameters related to in-situ horizontal stresses, elastic properties and strength properties, this paper focuses on the determination of elastic moduli from the pressure-volume curves obtained from a typical PMT test.

The discussions presented here only consider soil behavior under drained conditions. As such, the study is only applicable to silt and sand deposits with good drainage properties.

### 1.1 The pressuremeter modulus $E_0$

The analysis of stress and strain changes in a soil mass due to PMT loading is based in the theory of cavity expansion as it pertains to an infinitely long cylinder expanding into an infinite soil mass. Assuming uniform, isotropic, and linear-elastic soil behavior, the elastic properties of the soil are represented by the

pressuremeter modulus  $E_0$  (Briaud 1992), and is calculated with the following expression:

$$E_0 = (1 + \nu)(p_2 - p_1) \frac{\left(1 + \left(\frac{\Delta R}{R_0}\right)_2\right)^2 + \left(1 + \left(\frac{\Delta R}{R_0}\right)_1\right)^2}{\left(1 + \left(\frac{\Delta R}{R_0}\right)_2\right)^2 - \left(1 + \left(\frac{\Delta R}{R_0}\right)_1\right)^2} \quad (1)$$

where  $p$  and  $\Delta R/R_0$  are the pressure and the corresponding radial strain recorded at the beginning (subscript 1) and at the end (subscript 2) of the linear portion of the PMT pressure-volume curve, respectively. The Poisson's ratio is given by  $\nu$ . For soils under drained conditions, (i.e., zero excess pore-pressure), a Poisson's ratio of 0.33 is typically used, in which case the pressuremeter modulus is designated as the Menard's modulus  $E_M$  (Baguelin et al. 1978).

### 1.2 Young's modulus and PMT testing

It has long been recognized that the Menard's modulus  $E_M$  does not directly represent the Young's modulus  $E$  of the tested soils.

Menard and Rousseau (as reported by Briaud 1992), noted that using  $E_M$  as the elastic modulus of the soil resulted in

predicted footing settlements, which were consistently larger than actual measured settlements. To compensate for this over prediction of settlements, Menard and Rousseau suggested a correction factor, later designated as the Menard's  $\alpha$  factor, which helps to predict accurate quasi-elastic responses of soil masses undergoing loading. In their approach, the elastic modulus correlates to the Menard modulus using:

$$E = E_M / \alpha \quad (2)$$

Values of the  $\alpha$  parameter were determined empirically for different type of soils, and for different states of compaction and rheologies. Namely,  $\alpha$  varies between  $\frac{1}{4}$  and 1 (after Baguelin et al. 1978).

Briaud (1992) further researched the issue and listed a number of reasons contributing to the differences observed between the measured  $E_M$  and the elastic modulus  $E$ , namely:

- Modulus is measured over a rather large range of radial strains;
- Tension may develop near borehole walls, which may result in degradation of the average elastic modulus;
- Drilling and installation of the probe may cause soil disturbance near the borehole wall;
- Expression (1) assumes an infinite long cylinder, whereas PMT testing pressurizes a finite length of the borehole, thereby introducing errors in the determination of  $E_M$ ;
- PMT testing exerts a load pattern that lasts for several minutes; however actual foundation loadings act for much longer periods;
- Soil anisotropy may be present, thereby the measured horizontal moduli may be different than vertical moduli needed in settlement analyses.

These effects however cannot be easily quantified. Therefore, to date, no correction framework has been developed to obtain better predictions of the Young's modulus using PMT test results.

It is clear to the authors that all factors listed above influence, to a certain degree, the outcome on the inferred values of  $E_M$ . However, it is their view that the generation of non-uniform stress-strain fields developing during PMT loading has a major, more important, effect in the way the elastic modulus  $E_M$  is measured than those factors listed above.

Strain hardening behavior of cohesionless soils results in stronger degradation of the elastic modulus of the soil at higher stress/strain levels (Gomes Correia et al. 2004), even during the pseudo-elastic range of soil deformations. Portions of the soil near the borehole walls during PMT testing are strained and stressed to a higher degree than portions of the soils away from the wall, therefore values of the moduli are lower than those developing far from the borehole walls.

This concept can be visualized sooner in the response of a cohesionless soil sample tested under triaxial conditions, as illustrated in Figure 1 in a simplified manner. When using a linear elastic-perfectly plastic model (bi-linear model), the soil response to triaxial loading is shown with the solid line. The actual response of the soil undergoing strain-hardening is illustrated with the dashed line. Whether we use a tangent or a secant modulus, the actual soil response reflects the degradation of the elastic modulus at higher strain levels.

The effects of strain-hardening have also been recognized by Prévost (1975), Clarke (1995), Gomes Correia (2004), and others, as it pertains to the pseudo-elastic response of soil under PMT loading.

While PMT results reflect the actual behavior of the soil including strain hardening, the interpretation of  $E_0$  and  $E_M$  is

based on the assumption that the soil response is linear elastic, with a constant value of the Young's modulus throughout the soil mass being tested.

This is to say that while the PMT test captures the true behavior of the soil mass, the interpretation of the elastic modulus using the linear elastic assumption is not sufficiently accurate, and therefore differences between values of the Menard's and the Young's moduli originate in the interpretation rather than in the PMT test itself.

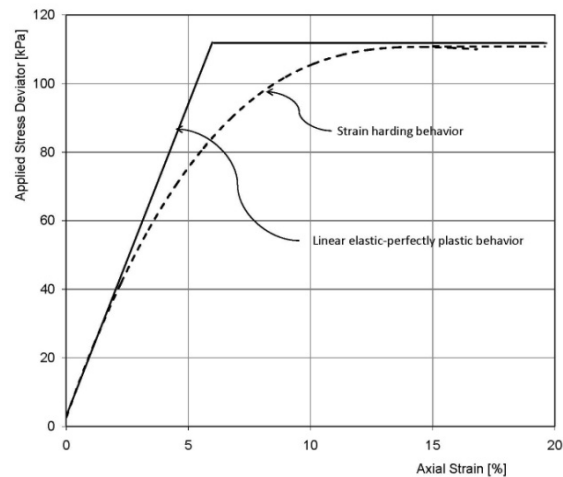


Figure 1. Triaxial test response

### 1.3 Young's modulus and the PMT reload modulus $E_R$

Mair et al. (1987), as well as others (Hughes 1977), have argued that disturbances during probe installation render values of initial shear moduli (or elastic moduli) unreliable, and that unload-reload moduli are more preferable. Geotechnical practitioners have met with success in predicting quasi-elastic deformation of soil-structure systems using finite element analysis with values of the PMT reload modulus  $E_R$  (Baker 2005). Typically, for cohesionless soils, the reload modulus is on the order of three times that of the Menard modulus  $E_M$ . Based on the author's practical experience, values of the reload modulus is often within the range of 2.0 to 4.0 times the value of  $E_M$ .

Using  $E_R$  as an equivalent of the Young's modulus however has no physical basis as the reload modulus is often measured from soil responses at stress and strains levels much higher than those stresses expected to develop under foundation loading. Furthermore, unload-reload cycles are usually completed after the yield pressure has been surpassed.

It should also be recognized that PMT loading imparts both deviatoric and volumetric stress, and some amount of consolidation takes place during the test. Given the fact that stresses during unload-reload cycles are much higher than in-situ stresses, it should be expected that at the end of the reload cycle the tested soil has changed, and it has now a stiffer behavior. This concept is supported by the fact that during PMT tests with multiple unload-reload cycles, the results show an increase of the reload moduli. For instance, the authors have observed PMT test results where, for dense sands, the reload modulus for the third cycle could be 25 % higher than that associated with the initial cycle. For loose or less compact sands the increase of reload moduli upon successive cycles is even higher. This phenomenon has also been reported by Mair

(1987) and Clarke (1995). As such, care must be exercised when predicting elastic deformations using values of  $E_R$  in finite elements analyses.

#### 1.4 Scope of present study

The main goal of this study is to explore the possibility of finding a working correlation between the Menard modulus  $E_M$  and the Young's modulus  $E$ .

For this purpose, a back-calculation approach was developed, in which soil responses under PMT testing were generated using finite element modeling, as follows:

- For a given set of initial subsoil conditions, including known values of in-situ stresses; Young's modulus; and strength parameters, the soil response under PMT loading is modeled using Finite Element Analyses (FEA);
- The predicted shape of the deformed membrane at the interface with the borehole is then extracted (data post-processing) for each individual load step;
- The volume expansion of such deformed membrane conditions is then calculated by explicit integration, thereby producing the typical *pressure vs. volume* ( $p$ - $v$ ) plot;
- Using PMT interpretation procedures, the Menard modulus is inferred from the post-processed  $p$ - $v$  plot; and
- A direct comparison between the assumed Young's modulus and the back-calculated Menard modulus is made.

The back-calculation process was repeated for a series of values of initial horizontal stress  $p_0$ , and Young's modulus  $E$ . In this parametric analysis, the relation between  $E$  and  $E_M$  was plotted for different values of  $p_0$ . This distribution was then used to generate a correlation between  $E$  and  $E_M$  for different values of in-situ stresses  $p_0$ .

A suggested correlation between  $E$  and  $E_M$  is thereby presented, which is intended to assist geotechnical practitioners using PMT test results and Finite Element Analyses to predict quasi-elastic deformation of soil-structures systems. Comparisons with the Menard's  $\alpha$  parameter are also attempted.

## 2 MODELING SOIL BEHAVIOR UNDER PMT TESTING

PMT loading imparts high levels of stress into the soil mass being tested. Depending on the state of compactness of a sandy deposit, peak pressures can vary from 400 kPa (loose state) to in excess of 8000 kPa (very dense state). For a particular test, the stress increase is maximum at the contact interface between the probe and the borehole walls, rapidly decreasing away from the borehole (Briaud 1992, Mair et al. 1987), resulting in non-uniform distributions of stresses and strains.

Once the  $p$ - $v$  response becomes non-linear, i.e., after applied pressure exceeds the yield pressure  $p_{yield}$ , portions of the soil near the borehole wall deform in the large-strain regime that includes yielding. Away from the borehole the soil still deforms in the small-strain regime in a quasi-elastic manner. In other words, once the stress increase exceeds the yield pressure, the stress-strain behavior of the soil mass becomes highly non-linear.

This type of non-linear elastoplastic phenomena in a soil mass exhibiting a wide range of strain/stress levels is very complex to analyze using any available mathematical formulation (Desai and Christian 1977; Potts and Zdravković 1999). Other Authors (Carter 1986; De Sousa-Coutinho 1990; Fahey 1993; Ladanyi 1998; Silvestri 2001 and 2009) investigating soil behavior under PMT testing have focused their attention to particular aspects of the responses and their

modeling. In each particular analysis, a set of assumptions is made to simplify the modeling of the particular aspect under scrutiny.

In this study a series of assumptions and working hypotheses are adopted with regards to the modeling of quasi-elastic soil responses under PMT loading, prior to yielding. These assumptions are listed in the discussion below.

#### 2.1 Basic aspects of the soil behavior

The most important aspects controlling the behavior of a cohesionless soil mass under PMT loading are:

- Stress dependency of elastic moduli, i.e., confining stress levels (Janbu 1963; Kolimbas et al. 1990); and
- Strain-hardening behavior during quasi-elastic deformations (Prévost et al. 1975; Clarke 1995).

Strength and dilatancy parameters are considered to control soil behavior on the post-yield stage of the PMT loading, but these do not have a significant impact during the quasi-elastic portions of PMT loading (Bolton 1986; Schanz et al. 1996).

For the analyses at hand, the following conditions are assumed:

- Rate of excess pore-pressure dissipation is faster than rate of PMT loading (drained conditions);
- At initial conditions the soil mass is considered to be continuum, uniform, and isotropic; and
- A value of the Poisson's ratio  $\nu = 0.3$  is representative of fully drained behavior of the cohesionless soil.

#### 2.2 Finite elements modeling

Soil deformation under PMT loading was modeled using the Hardening-Soil Model implemented into the Plaxis software (Plaxis 2D version 8 - Material Models Manual). This model considers Mohr-Coulomb failure criteria; stress-dependency of the elastic moduli; and deviatoric and volumetric hardening behavior due to both, shear and compressive strains, respectively. Soil dilatancy after Rowe's theory is also considered (Schanz et al. 1996 and 1999).

The PMT test geometry was discretized using a 2-dimensional axisymmetric configuration for a PMT probe with a length-to-diameter ratio of 6.5, typical of the RocTest NX-sized PMT probe.

Throughout the modeling the following intrinsic material properties were used:

Poisson's ratio	$\nu$	= 0.3
Effective angle of internal friction	$\phi'$	= 35°
Angle of dilatancy	$\Psi$	= 2°

This set of properties represents average values for cohesionless soils. In addition, a small amount of cohesion  $c' = 3$  kPa was adopted to prevent soil failure upon unloading, which the soil may experience near the borehole wall during drilling or pre-boring.

Regarding state properties, initial effective stresses were determined using the 'gravity loading' feature of Plaxis for geostatic stress conditions. In this approach, the effective horizontal stresses are generated for a effective unit weight  $\gamma_{eff} = \gamma_{sat} - \gamma_{water}$ , with an adopted value of  $\gamma_{sat} = 20$  kN/m<sup>3</sup>, and Poisson's ratio of 0.3. For the stress ratio (hardening parameter) a value of  $m = 0.5$  was assumed, which is a value representative for both sands and silts (Janbu 1963; Schmertmann 1986). The parameter  $m$  represents the stress-dependency of the elastic modulus on confining stress. The

failure ratio  $R_f = 0.9$  was adopted to represent both sands and silts.

A range of simulations were completed for different values of  $E$  and  $p_0$ , which is discussed in the following sections. Regarding the loading conditions the following stages were implemented:

1. Generation of in-situ initial stresses (gravity loading);
2. Borehole drilling (unloading);
3. PMT test (step-wise, monotonic loading at the probe-borehole interface).

The adopted PMT loading procedure was consistent with the pressure-controlled loading mode (stress-control procedure). This loading mode does not impose any constraints on the deformed shape of the PMT membrane.

### 3 FEA AND POST-PROCESSING RESULTS

#### 3.1 Menard modulus from predicted FE responses

The FEA modeling of the soil response provided vertical and radial displacements,  $\Delta v$  and  $\Delta R$ , throughout the soil mass at node locations for each pressure step. Based on the discretized geometry of the probe, a total of 33 nodes were located along the probe-soil interface.

The volume expansion  $v$  of the probe, as it would be observed by the test operator during actual test, was determined by data post-processing using the FEA displacements; i.e., by explicit integration of radial displacements over the length of the probe-soil interface. A particular volume increase  $v_i$  was determined for each pressure-step  $p_i$ . This set of data points was then plotted as the  $p$ - $v$  curve, which was subsequently used to determine the Menard modulus  $E_M$ .

To validate the Plaxis model and associated post-processing calculations, a benchmark problem was developed for the case of a pressuremeter test in a soil with an initial in-situ horizontal stress of  $\sigma'_{h0} = 100$  kPa, and Young's modulus  $E = 30$  MPa.

At first, the problem was analyzed using Plaxis Linear Elastic Soil model. The corresponding response and post-processed  $p$ - $v$  curve is illustrated in Figure 2 as the linear distribution. The interpreted value of the Menard modulus, i.e., using expression (1), yielded a back-calculated value of  $E_M = 31.6$  MPa. This is to say, had the soil behavior been truly linear elastic, the interpreted value of  $E_M$  would have been 5.3% higher than the actual Young's modulus, which is reasonably accurate for the boundary-valued problem at hand.

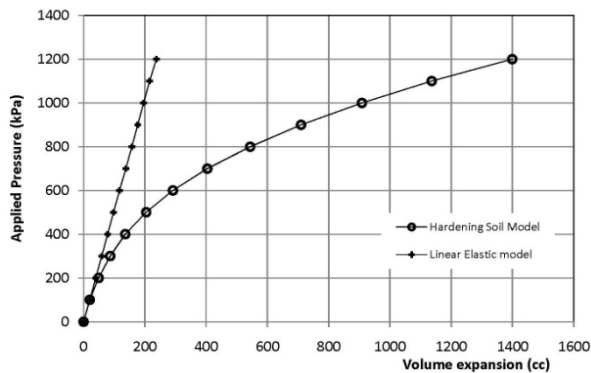


Figure 2. Pressuremeter  $p$ - $v$  responses from Plaxis modeling

The increased value of the interpreted  $E_M$  stems from the fact that the modeled PMT probe has a finite length with restrained

seals at both ends, whereas expression (1) assumes an infinitely long cavity expanding into the soil. The former case is physically less stiffer and less accurate, than the latter.

Under the same circumstances, but using the Hardening-Soil Model, the predicted soil response and associated  $p$ - $v$  curve is shown in Figure 2 with a curved line (data points are small circles), which is typical of an actual PMT test response. The interpreted Menard modulus using expression (1) was  $E_M = 24.4$  MPa.

This simple benchmark problem highlights, at least from a numerical modeling point of view, the importance of strain-hardening behavior under non-uniform distributions of stress and strain developing during PMT testing.

It should be mentioned that an additional simulation was carried out for a different set of strength parameters, namely  $\phi' = 30^\circ$  and  $\Psi = 5^\circ$ . No significant changes in the interpreted values of  $E_M$  were observed, suggesting that during the initial part of the PMT test the strength parameters do not play a significant role in the quasi-elastic responses of the soil being tested.

#### 3.2 Parametric approach and back-calculation

The relationship between the soil's Young's modulus and the inferred or back-calculated Menard modulus was generated for a set of parametric variables, namely the Young's modulus  $E$  and the in-situ initial horizontal stresses  $p_0$ .

In order to cover a practical range of in-situ horizontal effective stresses, the following values for  $p_0$  were used:

50; 100; 150; 200; and 350 kPa

which would approximately represent testing depths from 5 to 70 m below ground surface.

Regarding the in-situ undisturbed elastic moduli, the following values for  $E^{ref}_{50}$  were adopted:

5; 10; 15; 20; 30; 60; and 90 MPa

Plaxis Hardening-Soil model defines  $E^{ref}_{50}$  as the reference stiffness modulus, and the corresponding Young's modulus is determined with the following expression:

$$E = \frac{2 E^{ref}_{50}}{(2 - R_f)} \left( \frac{\sigma'_3}{p_a} \right)^m \quad (3)$$

This expression is valid for cohesionless soils (effective cohesion is zero or negligible). The reference pressure  $p_a = 100$  kPa is the atmospheric pressure. Furthermore, in the context of these discussions, the following simplification applies at initial conditions:

$$\sigma'_3 = p_0 = \sigma'_{h0} \quad (4)$$

where  $p_0$  refers to the effective initial pressure (also known as the effective contact pressure).

The failure ratio  $R_f = 0.9$  adopted for this study is consistent with a ductile type of failure typically exhibited by PMT test responses in most soils, including clays.

The basic correlation data between  $E$  and  $E_M$ , as generated with the back-calculation FEA approach is listed in Table 1 below. The inferred values of the Menard's  $\alpha$  parameter are also included in Table 1.

The relation between  $E$  and  $E_M$  is shown in Figure 3. In this graph it can be observed that  $E_M$  values associated with a  $p_0$  stress level lined up with an associated linear regression coefficient of  $R^2 = 1.00$ .

Regression analyses completed on the zero-intercept and slope values for each of the five distributions were further used to condense ( $E$ - $E_M$ ) data points into the following linearized expression:

$$E = a + b E_M \quad (5)$$

with

$$a = 3.90 p_a - 0.16 p_0 \quad (6)$$

and

$$b = 0.80 + 0.59 p_0/p_a \quad (7)$$

As mentioned above,  $p_a$  and  $p_0$  represent atmospheric and initial effective horizontal stresses, respectively. Expression (5) is dimensionally consistent, and either SI or Imperial units may be used with the same listed coefficients.

Plaxis Parameters			Back-calculation FE analyses			$\alpha$
$\sigma'_{ho}$	$E_{50}^{ref}$	$E$	$E_M$	$p_L^*$	$E_M/p_L^*$	
[kPa]	[MPa]	[MPa]	[MPa]	[kPa]	[-]	[-]
50	5	6.6	6.3	360	18	0.95
	10	13.3	11.9	510	23	0.90
	15	19.9	17.8	600	30	0.89
	20	26.5	23.6	740	32	0.89
	30	39.8	35.2	860	41	0.88
	60	79.6	70.5	1290	55	0.89
	90	119.4	105.1	1610	65	0.88
100	5	9.1	7.2	550	13	0.79
	10	18.2	14.0	640	22	0.77
	15	27.3	21.0	1000	21	0.77
	20	36.4	27.5	1110	25	0.76
	30	54.5	41.1	1450	28	0.75
	60	109.1	81.4	2060	40	0.75
	90	163.6	121.6	2560	48	0.74
150	5	11.0	7.9	720	11	0.72
	10	22.0	14.6	1060	14	0.66
	15	33.0	21.4	1270	17	0.65
	20	44.0	28.3	1480	19	0.64
	30	66.1	42.0	1670	25	0.64
	60	132.1	81.5	2570	32	0.62
	90	198.2	121.3	3000	40	0.61
200	5	12.6	7.7	1100	7	0.61
	10	25.3	14.0	1310	11	0.55
	15	37.9	20.2	1680	12	0.53
	20	50.5	26.4	1860	14	0.52
	30	75.8	39.0	2340	17	0.51
	60	151.6	76.5	3220	24	0.50
	90	227.4	114.0	4050	28	0.50
350	5	16.6	7.7	1240	6	0.46
	10	33.2	13.3	1860	7	0.40
	15	49.8	19.0	2290	8	0.38
	20	66.4	24.9	2460	10	0.38
	30	99.6	36.7	3480	11	0.37
	60	199.1	71.3	4900	15	0.36
	90	298.7	106.0	6100	17	0.35

Table 1. Correlation data between  $E$  and  $E_M$  moduli

It is noted that expressions (5) to (7) consider the soil mechanics sign convention, where compression is positive.

Also, based on the nature of the regression analysis, relative errors associated with expression (5) are between  $\pm 4\%$  (lower range of confining stresses  $p_0$ ) and  $\pm 0.5\%$  (higher range of  $p_0$ ).

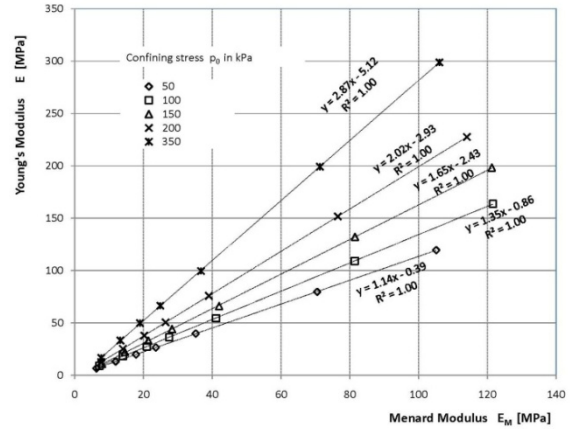


Figure 3.  $E_M$  and  $E$  correlation from parametric study

#### 4 MENARD'S $\alpha$ PARAMETER

Based on back-calculated values of  $E_M$ , the corresponding values of the predicted  $E_M/E$  ratio are included in Table No. 1. For stress confinement levels above 100 kPa these predicted ratios compare rather well with those values of the Menard's  $\alpha$  parameter for silts and sand, both under NC and OC conditions, namely  $1/3$ ,  $1/2$ , and  $2/3$  (Baguelin et al. 1978, Briaud 1992). Based on the present study, it appears that at lower confinement levels, i.e., lower than 100 kPa, cohesionless soils are less affected by the combined effect of strain-hardening and non-uniform strain-stress distributions, in which case Menard moduli may be similar to Young's moduli.

#### 5 CONCLUSIONS

The stress-strain behavior of cohesionless soils under PMT test conditions has been investigated using the finite element method. For saturated soils under drained conditions, an elasto-plastic hardening soil model was chosen to account for stress hardening of the soils, the stress-dependency of the elastic modulus and the non-linear, elasto-plastic deformations near the test cavity.

Based on this numerical study, and for the conditions listed above, the following observations are made:

- A relation between the Young's modulus  $E$  and the Menard pressuremeter modulus  $E_M$  is hereby proposed for cohesionless soils. Results from expression (5) compare well with empirical values of the Menard's rheological  $\alpha$  parameters for stress confinement above 100 kPa.
- The proposed relationship incorporates the effects of stress-dependency and strain-hardening via the contact pressure  $p_0$ , as it is obtained from PMT testing data.
- The probe's restrained ends have been taken into account by the boundary-valued problem, therefore the proposed correlation between  $E$  and  $E_M$  is applicable to mono-cell type of probes. By using this approach there is no benefit or improvement in using probes with guard-cells, which can be cumbersome to operate and difficult to repair in the field.
- Reload moduli  $E_R$  should not be used as the Young's moduli for silts or sands under confining stress levels

below 100 kPa as it could result in under-prediction of deformations or settlements.

In closing, given the nature of the numerical analysis of the present study, the relation between  $E$  and  $E_M$ , as suggested by expression (5), is strictly hypothetical. The authors however believe that if there exists a relation between  $E$  and  $E_M$ , it would have a form similar to that of expression (5).

## 6 ACKNOWLEDGEMENT

The Authors would like to express a heartfelt Thank You to Mr. Louis Marcil of Roctest (Montreal, Canada), to Dr. Dieter F.E.Stolle of McMaster University (Dep. Of Civil Engineering, Hamilton, Canada), and to Ms. Anne Bermingham of 2WA Consulting (Hamilton, Canada) for their help in the preparation of this paper.

## 7 REFERENCES

- Baguelin F., Jezequel J.F. and Shields D.H. 1978. The pressuremeter and foundation engineering. TransTech Publications.
- Baker C.N. 2005. The use of the Menard pressuremeter in innovative foundation design from Chicago to Kuala Lumpur (Paper and ensuing discussion by Attendants). Published in ISP5-Pressio 2005, International Symposium – 50 years of pressuremeters. Edited by Gambin M., Magnan J.P. and Mestat P. Laboratoire Central des Ponts et Chaussées.
- Bolton M.D. 1986. The strength and dilatancy of sands. *Géotechnique* 36, No.1, 65-78.
- Briaud J.L. 1992. The pressuremeter. Balkema.
- Carter J.P., Booker, J.R. and Yeung S.K. 1986. Cavity expansion in cohesive frictional soils. *Géotechnique* 36, No. 3, 349-358.
- Clarke B.G. 1995. Pressuremeters in geotechnical design. Taylor & Francis.
- Desai C.S. and Christian J.T. 1977. Numerical methods in geotechnical engineering. McGraw-Hill.
- De Sousa Coutinho A.G.F. 1990. Radial expansion of cylindrical cavities in sandy soils: Application to pressuremeter tests. *Canadian Geotechnical Journal*, 67, 737-748.
- Fahey M. and Carter J.P. 1993. A finite element study of the pressuremeter test in sand using a nonlinear elastic plastic model. *Canadian Geotechnical Journal* 30, 348-362.
- Gomes Correia A., Antão A. and Gambin M. 2004. Using a non linear constitutive law to compare Menard PMT and PLT E-moduli. Proceedings of the International Conference on Site Characterization, 2, Porto, Portugal, Vol. 1, 927-933.
- Hughes J.M.O., Wroth C.P. and Windle D. 1977. Pressuremeter tests in sands. *Géotechnique* 27, No.4, 455-477.
- Janbu N. 1963. Soil compressibility as determined by oedometer and triaxial testing. Proc. Of the European Conference of Soil Mechanics and Foundation Engineering. Wiesbaden, Germany. 1: 19-25.
- Kolymbas D. and Wu W. 1990. Recent results of triaxial tests with granular materials. *Powder Technology*, 60. 99-119.
- Ladanyi B. and Foriero A. 1998. A numerical solution of cavity expansion problem in sand based directly on experimental stress-strain curves. *Canadian Geotechnical Journal* 35, 541-559.
- Mair R.J. and Wood D.M. 1987. Pressuremeter testing: Methods and interpretation. Butterworth-Heinemann.
- Potts D.M. and Zdravković L. 1999. Finite element analysis in geotechnical engineering – Theory. Thomas Telford.
- Prévost J.-H and Hoek K. 1975. Analysis of pressuremeter in strain-softening soil. *Journal of Geotechnical Engineering Div. ASCE*. 101 GT8.
- Silvestri V. 2001. Interpretation of pressuremeter tests in sand. *Canadian Geotechnical Journal* 38, 1155-1165.
- Silvestri V., Abou-Samra G. and Bravo-Jonard C. 2009. Effect of flow rules and elastic strains on pressuremeter test results in dense sand. *Canadian Geotechnical Journal* 46, 160-167.
- Schanz T. and Vermeer P.A. 1996. Angles of friction and dilatancy of sand. *Géotechnique* 46, No. 1, 145-151.
- Schanz T., Vermeer P.A. and Bonnier P.G. 1999. The Hardening-Soil model: Formulation and verification. Published in *Beyond 2000 in Computational Geotechnics*. Editor: R.B.J. Brinkgreve. A.A. Balkema.
- Schmertmann, J.H., 1986. Dilatometer to Compute Foundation Settlement, *Use of In Situ Tests in Geotechnical Engineering*, Editor: Samuel Clemence, pp. 303-320